$$\dot{V}_{dc} = -\frac{1}{C_s}\left(\frac{P_{ac}}{V_{dc}} + G_s V_{dc}\right) \quad (3)$$

where,

$$P_{ac} = V_{di} I_d + V_{qi} I_q = \text{real}(V_i I_s^*) \quad (4)$$

The d-q STATCOM's bus voltage components related to the infinite bus are:

$$\left.\begin{aligned} V_{sd} &= V_{bd} + I_{td} R_{sb} - I_{tq} X_{sb}\left(1+\frac{\omega}{\omega_o}\right) + \dot{I}_{td} L_{sb} \\ V_{sq} &= V_{bq} + I_{td} X_{sb}\left(1+\frac{\omega}{\omega_o}\right) + I_{tq} R_{sb} + \dot{I}_{tq} L_{sb} \end{aligned}\right\} \quad (5)$$

where, $X_s=X_{trans}$, $R_s=R_{trans}$, $Z_{trans}= R_{trans}+ jX_{trans}$, $I_t= I_g + I_s$, and $I_t= I_{td} + jI_{tq}$.

Due to the fact that the STATCOM is placed on high-voltage transmission lines a step-down transformer is required in order to allow the use of power electronics devices as shown in Fig.1. The relationships between the converter DC and AC sides are obtained by applying the Pulse Width Modulation (PWM) technique, the VSC allows representation of the STATCOM with a voltage at fundamental frequency as:

$$V_i = c\, V_{dc} \angle \phi \quad (6)$$

where c is the amplitude modulation ratio of the VSC.

2.1.2 SCG Model

The SCG is a low inertia unit so, it is equipped with fast valving routine to improve its stability [18]. The IEEE technical committee report illustrates the various models that represent the turbine dynamics. The SCG's mathematical model is described in [19]. Based on Park's model used *d-q axes* transformation, The system nonlinear first-order differential equations are:

$$\dot{\delta} = \omega \quad (7)$$

$$\dot{\omega} = \frac{\omega_o}{2H}(T_m - T_e) \quad (8)$$

$$\dot{\psi}_d = \omega_o\left(V_{sd} + I_{gd}(R_a+R_{gs}) + \psi_q\right) + \omega\,\psi_q \quad (9)$$

$$\dot{\psi}_q = \omega_o\left(V_{sq} + I_{gq}(R_a+R_{gs}) - \psi_d\right) - \omega\,\psi_d \quad (10)$$

$$\dot{\psi}_{D1} = -\omega_o\, I_{D1}\, R_{D1} \quad (11)$$

$$\dot{\psi}_{Q1} = -\omega_o\, I_{Q1}\, R_{Q1} \quad (12)$$

$$\dot{\psi}_{D2} = -\omega_o\, I_{D2}\, R_{D2} \quad (13)$$

$$\dot{\psi}_{Q2} = -\omega_o\, I_{Q2}\, R_{Q2} \quad (14)$$

$$\dot{\psi}_f = \omega_o\left(V_f - I_f\, R_f\right) \quad (15)$$

The currents are obtained as a function of flux linkages as:

$$\begin{bmatrix} I_f \\ I_{gd} \\ I_{D1} \\ I_{D2} \end{bmatrix} = \begin{bmatrix} X_f & -X_{fd} & X_{fD1} & X_{fD2} \\ X_{fd} & -(X_d+X_{gs}) & X_{dD1} & X_{dD2} \\ X_{fD1} & -X_{dD1} & X_{D1} & X_{D1D2} \\ X_{fD2} & -X_{dD2} & X_{D1D2} & X_{D2} \end{bmatrix}^{-1} \begin{bmatrix} \psi_f \\ \psi_d \\ \psi_{D1} \\ \psi_{D2} \end{bmatrix} \quad (16)$$

and

$$\begin{bmatrix} I_{gq} \\ I_{Q1} \\ I_{Q2} \end{bmatrix} = \begin{bmatrix} -(X_q+X_{gs}) & X_{qQ1} & X_{qQ2} \\ -X_{qQ1} & X_{Q1} & X_{Q1Q2} \\ -X_{qQ2} & X_{Q1Q2} & X_{Q2} \end{bmatrix}^{-1} \begin{bmatrix} \psi_q \\ \psi_{Q1} \\ \psi_{Q2} \end{bmatrix} \quad (17)$$

where,

$$T_e = \psi_d i_{gq} - \psi_q i_{gd} \quad (18)$$

2.1.3 Turbine and Governor System Model

The mathematical model of the governor and turbine system is represented by a set of first order differential equations as shown in Fig.3. Each stage in the mechanical system is represented by a first order differential equation and the hydraulic valves limits are imposed on the valves position and velocities [8].

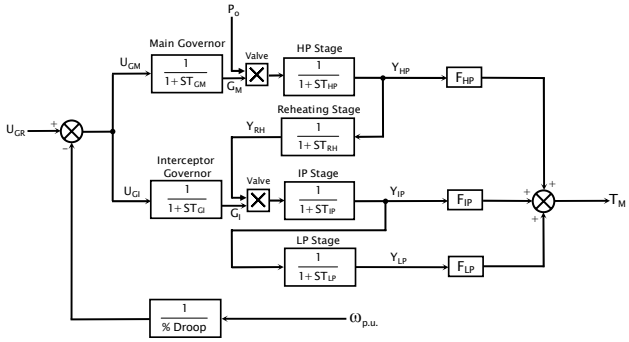

Fig.3 Representation of turbine and governor system

The mathematical model of the governor and turbine system is represented by a set of first order differential equations as:

$$\dot{G}_M = \frac{U_{GM} - G_M}{T_{GM}} \quad (19)$$

$$\dot{G}_I = \frac{U_{GI} - G_I}{T_{GI}} \quad (20)$$

$$\dot{Y}_{HP} = \frac{G_M P_o - Y_{HP}}{T_{HP}} \quad (21)$$

$$\dot{Y}_{RH} = \frac{Y_{HP} - Y_{RH}}{T_{RH}} \quad (22)$$

$$\dot{Y}_{IP} = \frac{G_I Y_{RH} - Y_{IP}}{T_{IP}} \quad (23)$$

$$\dot{Y}_{LP} = \frac{Y_{IP} - Y_{LP}}{T_{LP}} \quad (24)$$

The mechanical torque is given by:

$$T_m = F_{HP} Y_{HP} + F_{IP} Y_{IP} + F_{LP} Y_{LP} \quad (25)$$

The valves' velocities limits are based on the time required to reach the valves positions to 100% which is 150 ms [19]:

$0 \le G_M \le 1, \quad -6.7 \le \dot{G}_M \le 6.7 \quad$ and $\quad 0 \le G_I \le 1, \quad -6.7 \le \dot{G}_I \le 6.7.$

After the initial conditions calculation step from the phasor diagram shown in Fig.4, a digital MATLAB-SIMULINK model has been built to simulate the studied power system. The system non-linear equations are solved using Runge-Kutta integration technique with integration step 0.2 ms and the system is tested after normal operation period of 200ms. The SCG, the STATCOM, the transmission and the mechanical system parameters are mentioned in Appendix A.

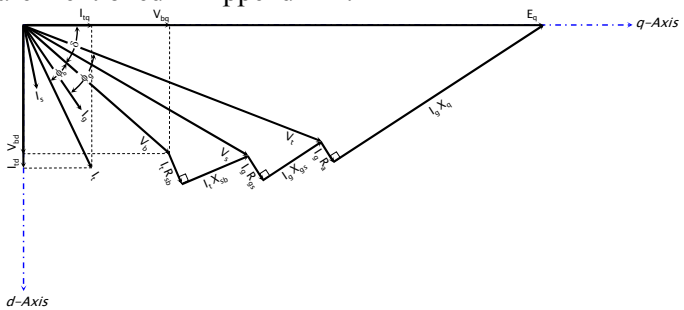

Fig.4 Phasor diagram of power system including a STATCOM device

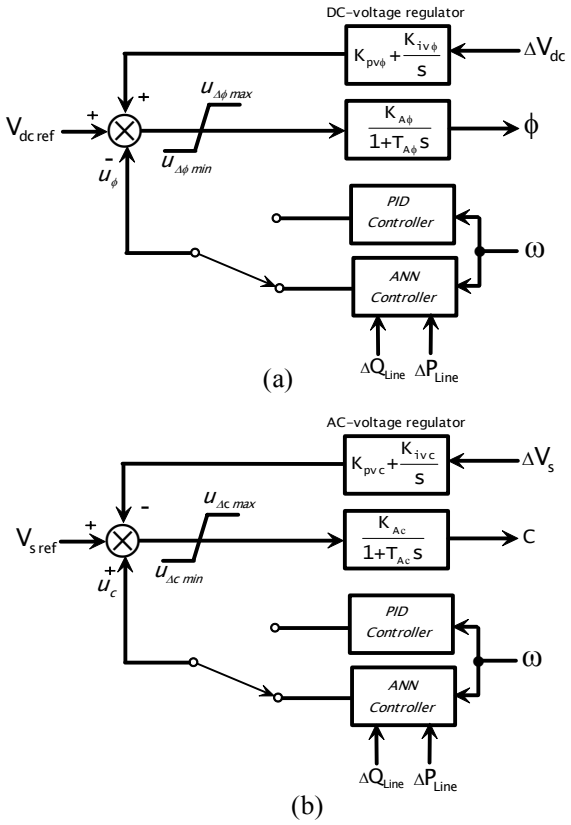

Fig.5 The STATCOM control systems
(a) phase control (b) Magnitude control

2.2 SCG CONTROL system

The performance of the SCG is improved by incorporating controllers in the governor loop such as phase advance network or PID controller [19]. The used controller in this paper is the PID controller whose parameters are determined using pole placement technique and these values are reported in Appendix A [20].

2.3 STATCOM CONTROL systems

One of the major reasons for installing a STATCOM is to improve dynamic voltage control and thus increases system load-ability and enhances the transient stability. The STATCOM is equipped either by conventional controller such as lead-lag or adaptive controller such as ANN controller to set the modulation ratio and the phase angle and hence the STATCOM output voltage magnitude and phase. In this study, the conventional controller used is the PID and the adaptive one is the ANN, selector has been employed to connect the desired controller to the STATCOM as shown in Fig.5.

2.4Conventional PID-STATCOM Controller

The PID controller is relatively simple in practical implementation and can enhance the system performance particularly to minimize post fault oscillations. Pole placement technique is used in order to determine the controller parameters [21].

The selected roots are the SCG's dominant roots at lagging p.f. of the system time invariant model. The dominant eigenvalues of the system with PID-STATCOM compared with the STATCOM-voltage regulators only are illustrated in Table 1. The results illustrate the voltage regulators add a negative damping, as the dominant roots are worse than the system without STATCOM. The objective of the damping control systems is concentrated on the movement of these modes towards the left-hand side of the s-plane. From the pole placement technique the STATCOM regulators and controllers are listed in Appendix A.

Table 1 The system dominant eigenvalues

At lagging p.f.			
Modes	Without STATCOM	PI_ϕ and PI_c-regulators	PID_ϕ and PID_c
Rotor	-4±j13	-3.96 ± j14.28	-5.5 ± j11
Field	-0.00147	-0.0015047	-0.001503

2.5 ANN NETWORK controller design

The conventional PID controller is designed according to a certain operating point and its parameters are fixed. To overcome the drawbacks of conventional controllers, ANN strategies are proposed due to its simple structure, adaptability, robustness and considering the power grid nonlinearities. To obtain the optimal values of ANN based PID controller parameters, two ANNs are established to take the place of PID_ϕ and PID_c damping controllers. The inputs to the ANNs are the deviation in the transmission line active and reactive powers and its output is only one PID parameter. So, the proposed ANN construction is repeated three times for each controller parameter (three for PID_ϕ and three for PID_c).

Fig.6 shows the construction of one network of these ANNs group, which consists of one input layer, one hidden layer (3-neurons) with a hyperbolic tangent sigmoid activation function and one output with a pureline activation function. The complete ANN controller system is illustrated in Fig.7.

The ANNs' weights and biases are adjusted by minimizing the system performance index, which indicates the systems' deviations. The system performance index (J), which is the total sum of the system deviations multiplied by the square of the time as:

$$J=\int_0^\infty e(t)*t^2 \qquad (26)$$

where, e(t) =Σ{deviations in δ, ω, valve position, $|V_t|$, V_{dc}, and $|V_s|$}, t: is the time.

The minimization of the performance index is implemented by the use of MATLAB optimization toolbox.

2.6 Eigenvalues Analysis

To demonstrate the effect of ANN-STATCOM controllers on the eigenvalues, The system is linearized using the system SIMULINK model. The system dominant eigenvalues with ANN-STATCOM compared with the PID-STATCOM are illustrated in Table 2. It can be concluded from table, the introduction of ANN-STATCOM controllers increase significantly the system damping.

Table 2 The system dominant eigenvalues

At lagging p.f.		
Modes	PID-STATCOM controllers	ANN-STATCOM controllers
Rotor	-5.5 ± j11	-9.47087±j10.2629
Field	-0.0015034	-0.0015035

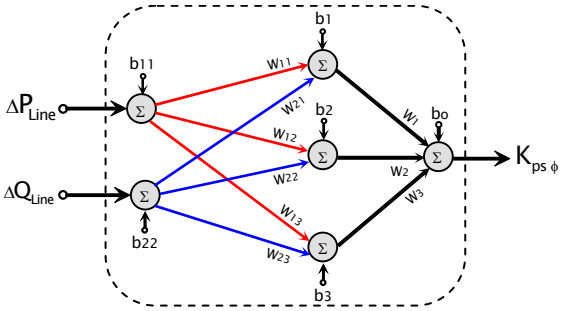

Fig.8 The architecture of one ANN

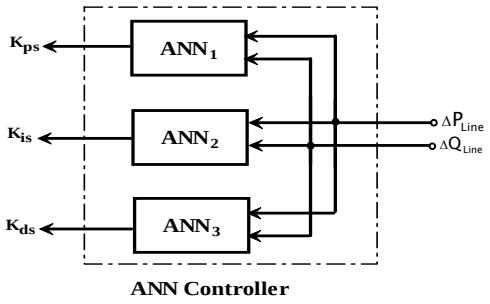

Fig.7 The ANN controller with all components

2.7 SMIB SIMULATION RESULTS

To study the robustness characteristics of the designed ANN-STATCOM damping controllers to all the operating conditions, simulation tests have been carried out using MATLAB-SIMULINK model of the system. The system performance is examined for various types of disturbances at different operating conditions. The simulation results are obtained in comparative form with conventional PID-STATCOM controllers. The system's time response for a symmetrical three-phase short circuit at one line of close to the infinite bus for 120 ms duration is shown in Fig.8. Starting from Fig 9 the results are focused on the comparison between ANN-STATCOM and conventional PID-STATCOM controllers. The time response of the system when the SCG is equipped by speed governor only for a symmetrical three-phase short circuit for 120 ms duration is shown in Fig.9. Fig. 10 shows the effectiveness of ANN-STATCOM to restore the system to its normal state after a major fault is applied. the System response to 3-phase short circuit followed by one line outage is shown in Fig.11. From Fig.12 to Fig.14 the system dynamic response is illustrated for 10% step increase U_{GR}, $V_{s\ ref}$, $V_{dc\ ref}$ for 200 ms. These results illustrate that the ANN-STATCOM controllers is more reliable than conventional controllers as it provides a good damping to the electro-mechanical modes of oscillations and all system variables quickly return to their initial values.

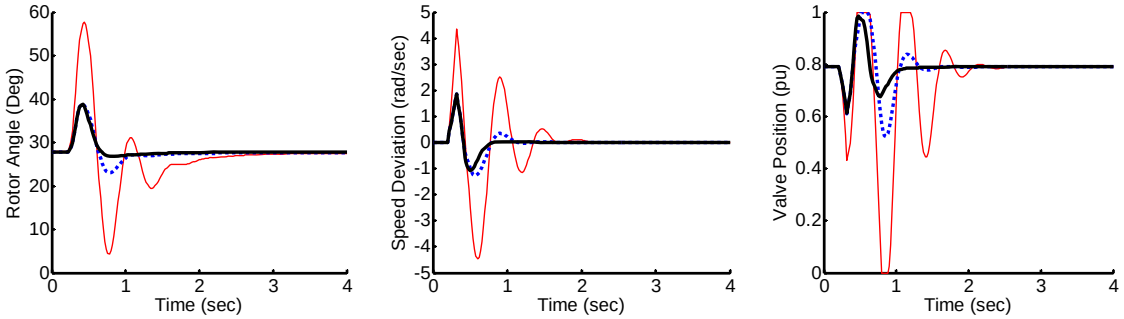

(a) Lagging p.f.

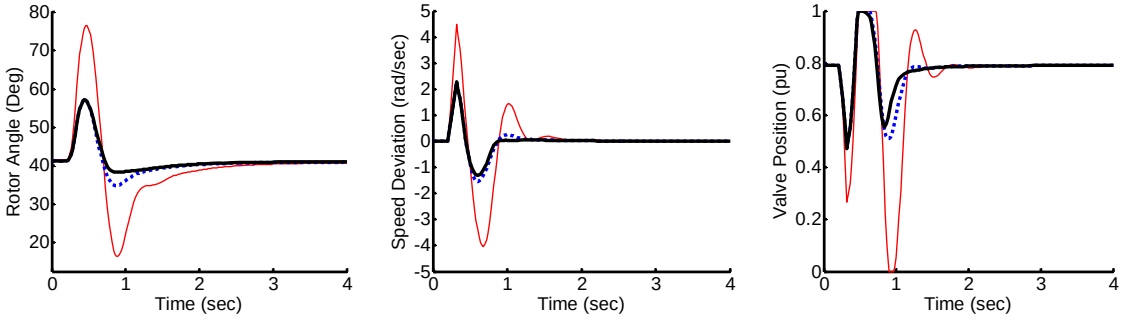

(b) Unity p.f.

Fig.8 System response to a 3-phase short circuit for 120 ms, SCG equipped with PID controller

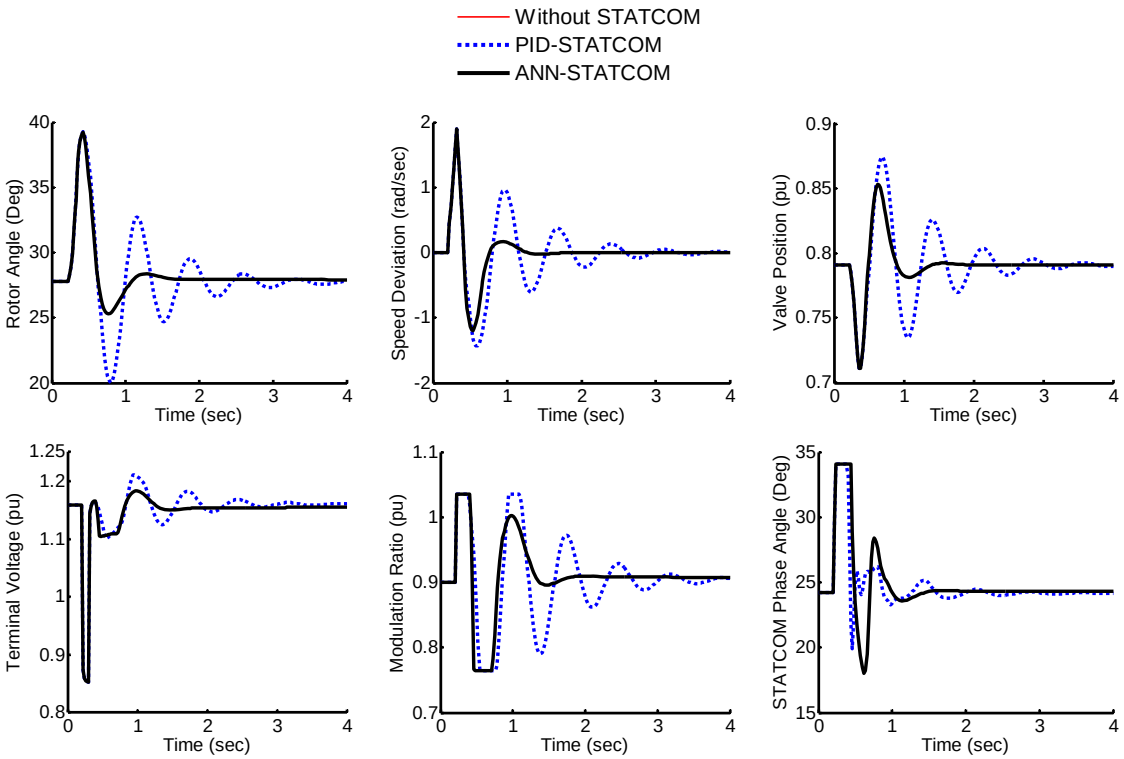

Fig.9 System response to a 3-phase short circuit for 120 ms at lagging p.f., SCG equipped with speed governor only

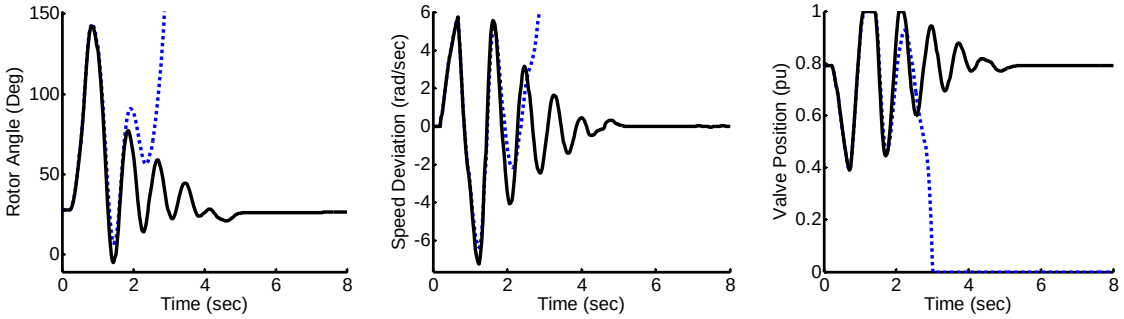

Fig.10 System response to a 3-phase short circuit for 490 ms at lagging p.f., SCG equipped with speed governor only

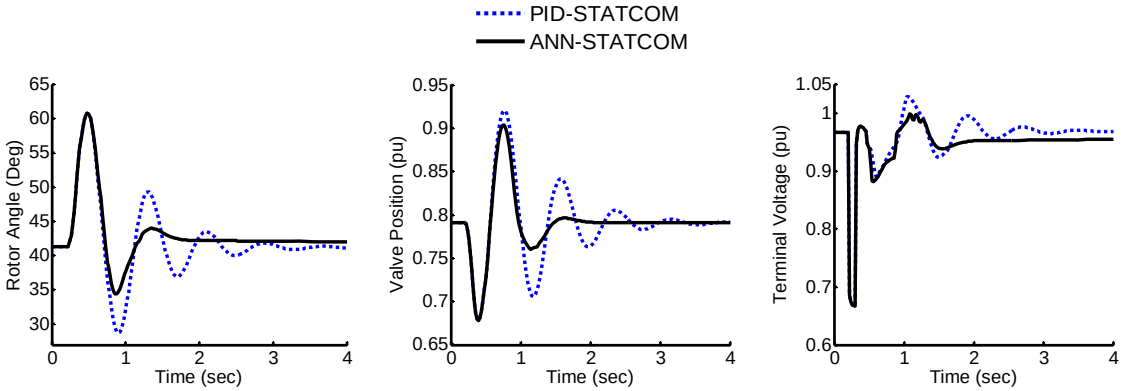

Fig.11 System response to 3-phase short circuit for 120 ms followed by one line outage for 200 ms at Unity p.f., SCG equipped with speed governor only

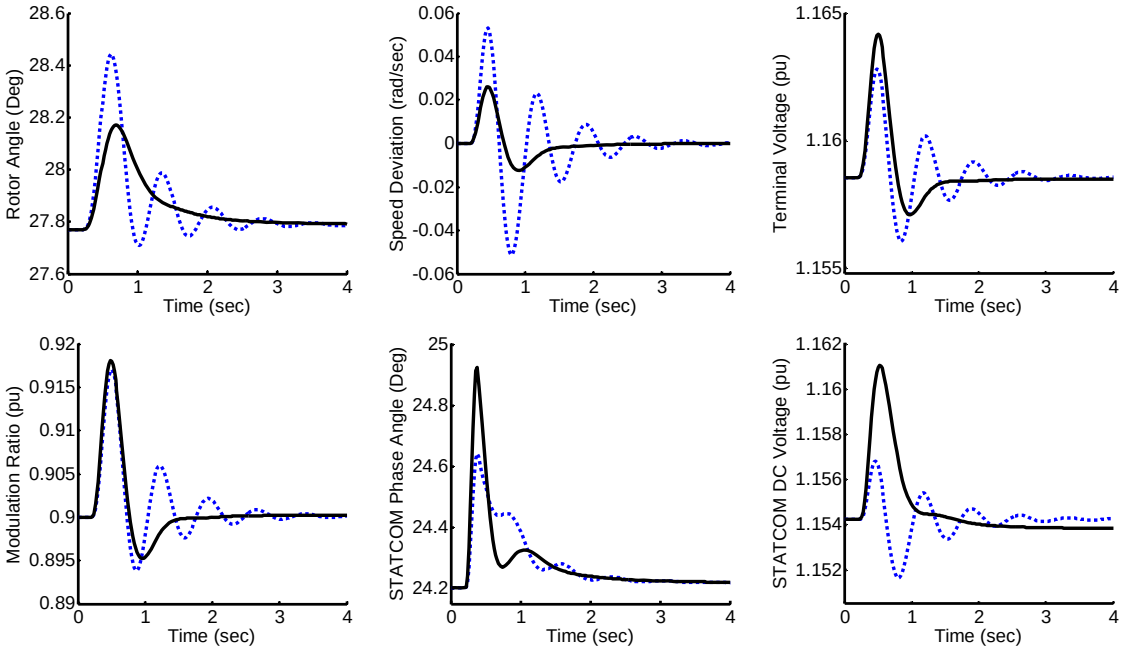

Fig.12 System response to a 10% step increase in mechanical input for 120 ms at lagging p.f. , SCG equipped with speed governor only

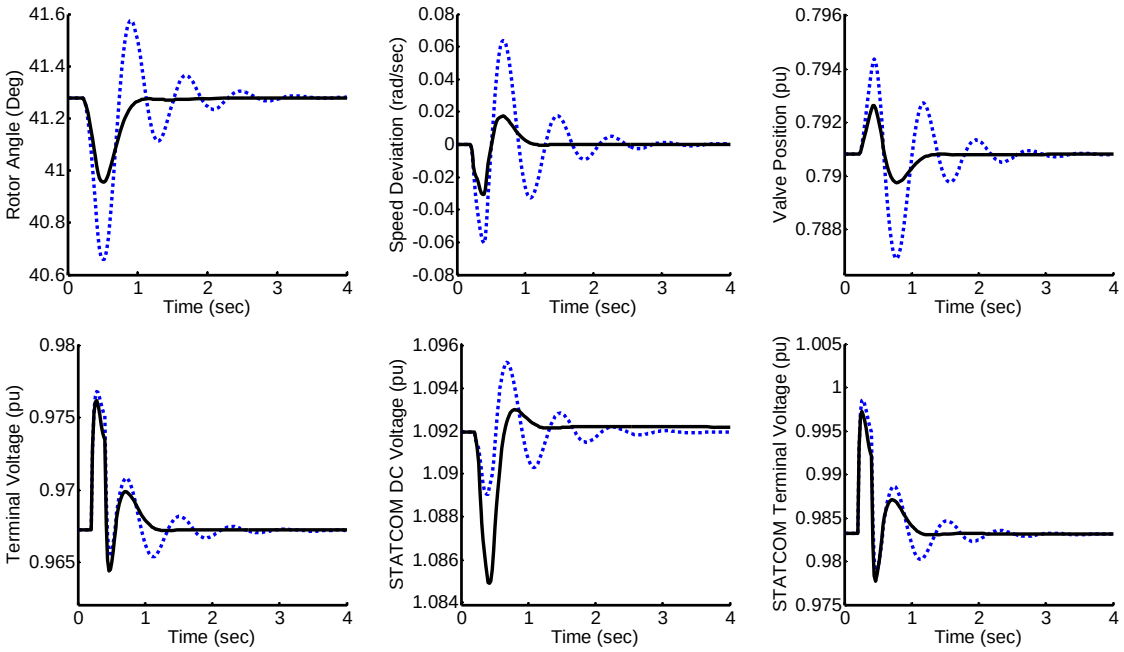

Fig.13 System response to a 10% step increase in $V_{s\,ref}$ for 200 ms, at unity p.f.

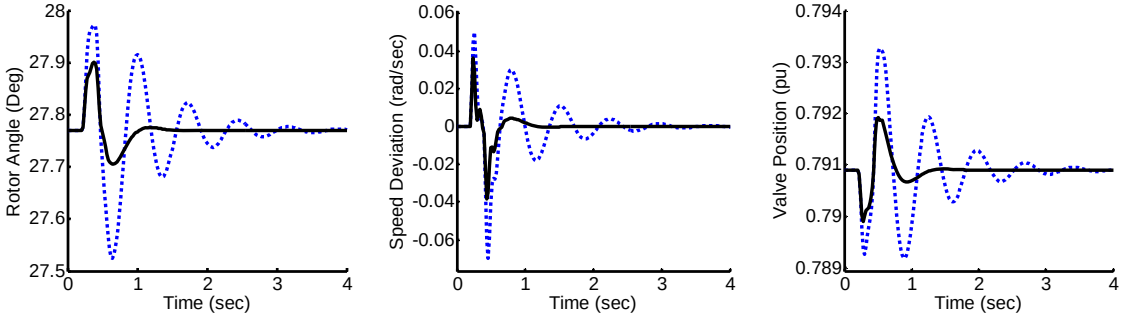

Fig.14 System response to a 10% step increase in $V_{dc\,ref}$ for 200 ms, at lagging p.f.

PID-STATCOM
ANN-STATCOM

3. Multi-Machine Power System

To verify the performance of the proposed ANN-STATCOM controller, a multi-machine power system is considered. The studied multi-machine power system is the New England power system: 10 machines, 39 buses and 19 load areas [22]. The single line diagram of the studied power system is represented in Fig.15. All loads treated as lumped impedances and the transmission system is expressed as nominal π double-circuit lines. The generating units are different types and ratings, nine conventional units and a SCG unit, as illustrated in Table 3. The generating units parameters are listed in Appendix A. In view of modeling, the conventional generating unit are represented by its reduced third-order model. However, a detailed representation for the SCG, STATCOM, control systems, and transmission lines are considered. The system generating units are equipped with various types of exciters as slow and fast acting thyristor exciters with different ceiling voltages.

3.1 Conventional Generators

Based on park's d-q axes, a third-order nonlinear mathematical model representation is established to represent each conventional machine. The differential equations are arranged as a set of first order equations as following [23]:

I- Mechanical equations:

$$\dot{\delta}^i = \omega^i \tag{27}$$

$$\dot{\omega}^i = \frac{\omega_o}{2H^i}(T_m^i - T_e^i - K_d^i\,\omega^i) \tag{28}$$

$$\dot{E}_q^{'i} = \frac{1}{T_{do}^{'i}}(E_{fd}^i - I_d^i(X_d^i - X_d^{'i}) - E_q^{'i}) \tag{29}$$

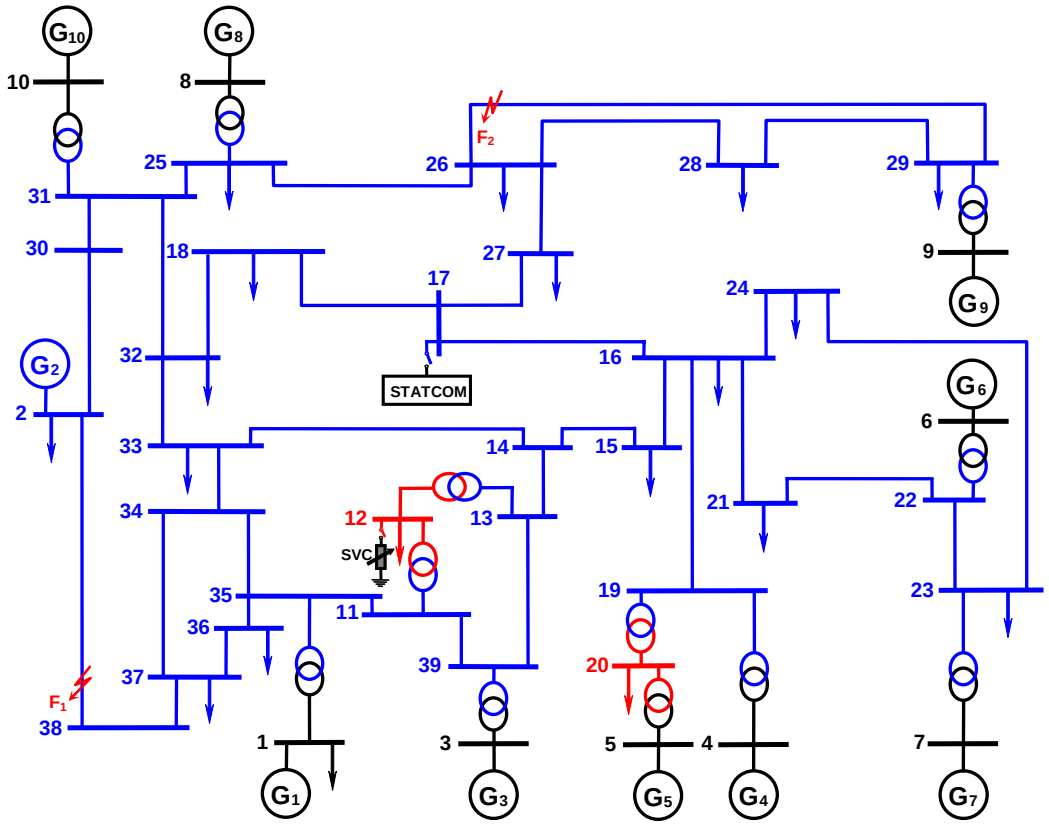

Fig.15 Single line diagram for the New England power system

Table 3 The generating units' arrangement

Generator No.	Type	Rating (MVA)	Generator No.	Type	Rating (MVA)
1	Nuclear	920.35	6	Steam	896
2	SCG	2000	7	Steam	835
3	Steam	835	8	Hydro-Electric	615
4	Steam	835	9	Nuclear	1070
5	Hydro-Electric	615	10	Steam	410

where,

$$T_e^i = E_q^{'i} I_q^i - I_d^i I_q^i (X_d^{'i} - X_q^i) \quad (30)$$

To reduce the system order, the mechanical input torques are assumed to be fixed for conventional machines. In this study, conventional generators are controlled via typical excitation systems using Various types of exciters with different ceiling voltages. In this control scheme the generators 1 and 6 are equipped with fast acting thyristor exciters with negligible time lag. The other conventional machines are equipped with rotary exciter types. High gains automatic voltage regulators (AVRs) are used with the exciters to control the generators' terminal voltages. The block diagram of the excitation systems for conventional generators is shown in Fig.16. The excitation system parameters are listed in Appendix-A according to the IEEE standardization.

Under heavy load conditions the continuously acting of excitation systems produce a negative damping to the system oscillations. To eliminate this undesired effect and in general to improve the system damping, an artificial network producing torque in the speed phase is introduced. The network used to add a signal that control the synchronous machine terminal voltage is called power system stabilizer (PSS) network [24]. The PSS is a lead-lag network with two time constants T_1 and T_2 and gain G_s. The PSS attached to the excitation system is shown in Fig.16. The PSS transfer function is given by:

$$\frac{y_s}{\omega} = G_s \frac{1+T_1 s}{1+T_2 s} \quad (31)$$

where, y_s is the control signal, and ω is the deviation in machine speed. The ratio T_1/T_2 is 10 [24]. A number of iterations have been taken to obtain the suitable gains for PSS for different generating units. Parameters of excitation systems and PSSs for conventional generating units are listed in Appendix A

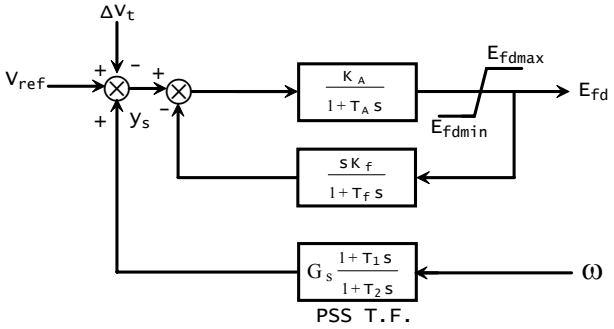

Fig.16 Excitation system for conventional generating units

3.2 Optimal Location of STATCOM

STATCOM is placed at a suitable bus to enhance the power system stability and to improve the damping characteristics of the power system. The system performance index technique is applied to choose the optimal location. The power system transient performance is obtained when it is subjected to a 3-phase short circuit. Fig.17 shows the values of performance index for different buses location when the STATCOM is equipped with PID controller with feedback signal of the speed deviations for all generators. According to the values of performance index, the optimal location for the STATCOM is bus 30.

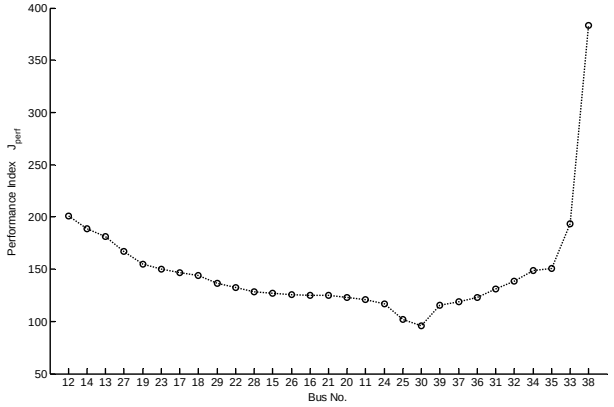

Fig.17 The system's performance index versus the STATCOM location

3.3 Multi-Machine Power System Simulation Results

The time response of the studied multi-machine power system involving a STATCOM is illustrated when it is subjected to different disturbances. The STATCOM-based stabilizers (PID and ANN) parameters are optimally designed when coordinated with the power system controllers by the help of MATLAB optimization techniques.

The generators' rotor angles and the SCG valve position are used to evaluate the effectiveness of the proposed nonlinear model-based optimization process. The simulation results are obtained in a comparative form to show the positive effect of the ANN-STATCOM on the system performance.

Fig.18 shows the response when the system is subjected to a 3-phase short circuit at F_1. This figure illustrates the significant improvement of the system's performance resulting from adding the STATCOM as it adds more damping. For Fig.19, the comparison is focused on the effect of STATCOM-controllers only. The figure shows that, the system's response with ANN-STATCOM is more damped. So, all system variables return to their initial values quickly in case of ANN-STATCOM compared with PID-STATCOM. Fig.20 and Fig.21 show the dynamic response of the system such as 10% increase in U_{GR} or load increase. These results confirm the ability of ANN-STATCOM to increase the system's damping.

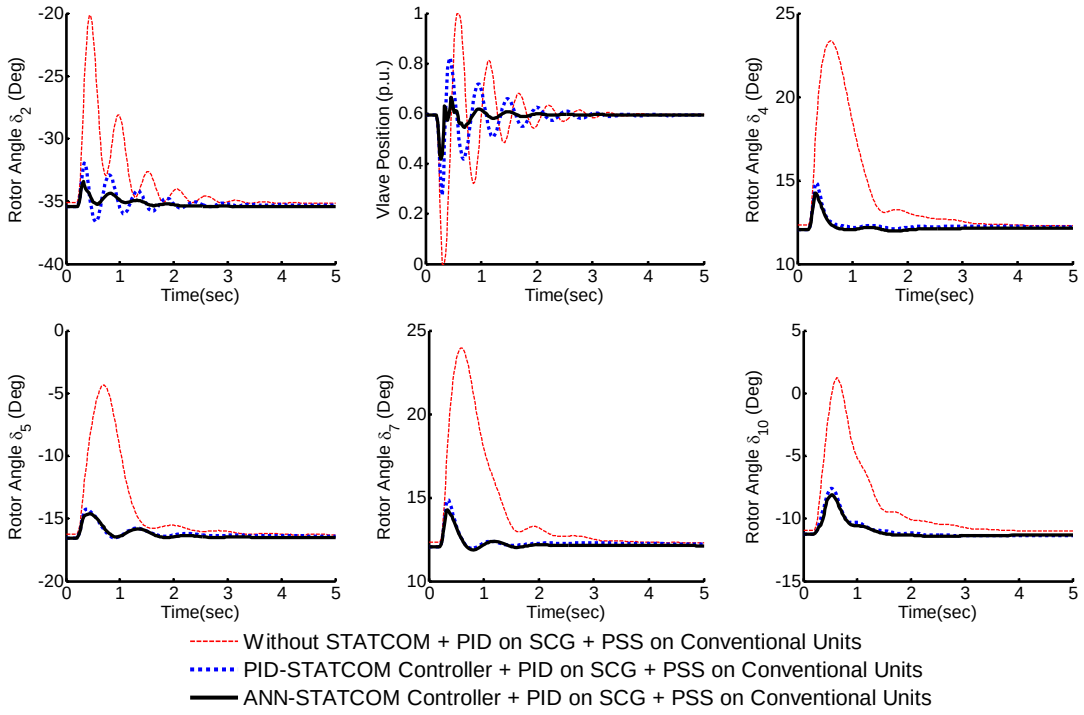

Fig.18 System transient response to a 3-phase short circuit for a 100 ms at F_1

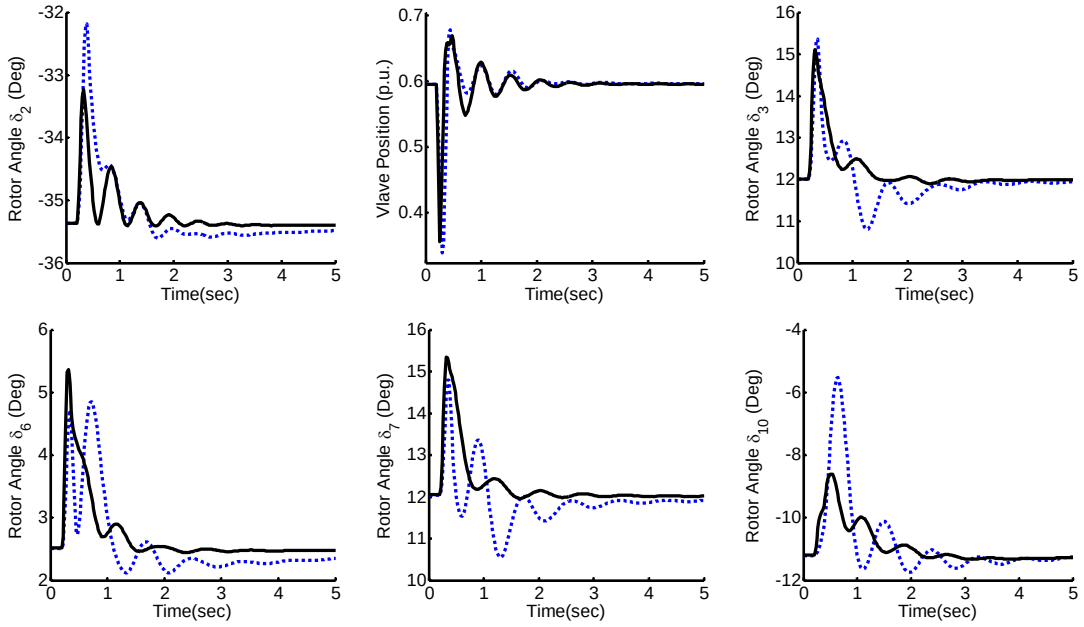

Fig.19 System transient response to a 3-phase short circuit for a 100 ms at F_2

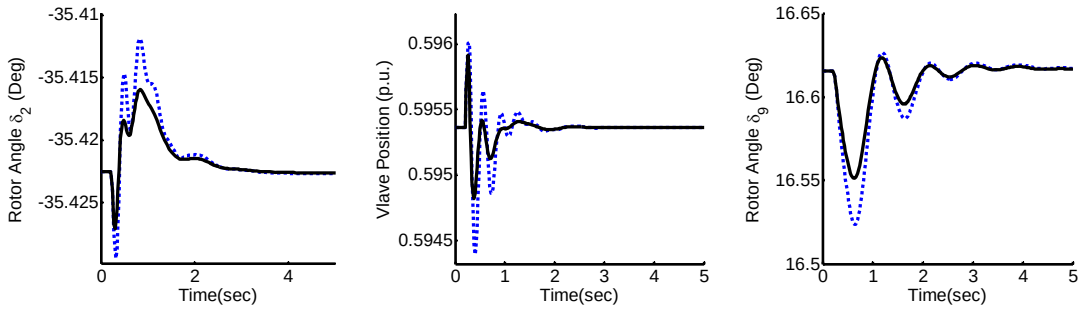

Fig.20 Dynamic response to a 10% load increase at bus 16 for 100 ms

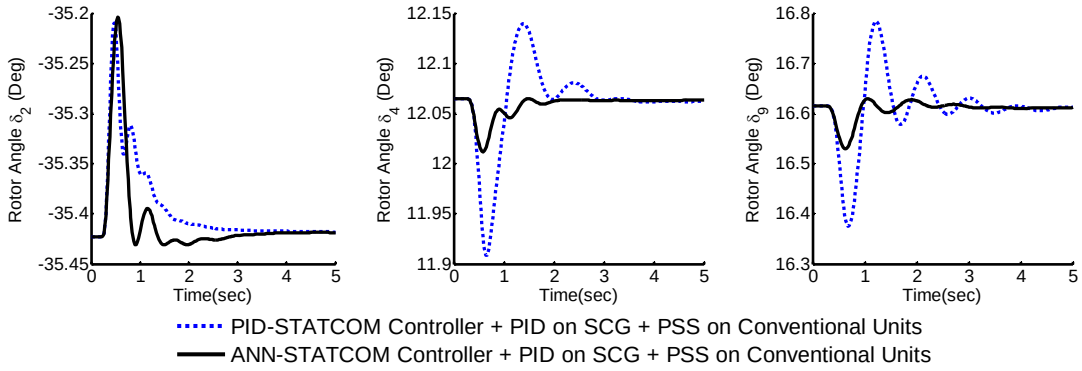

Fig.21 Dynamic response to 10% increase in SCG mechanical input for 100 ms

.

4. CONCLUSION

This paper presents the design of the ANN-STATCOM $_{controllers}$ based PID-STATCOM for stabilization the power systems. The control strategy has been implemented on a STATCOM attached to a SMIB and the New England power systems. In this study the SCG is equipped with PID controller in the governor loop and other units are equipped with PSS. For SMIB, the PID-STATCOM is designed using pole-placement technique. However, in case of multi-machine power system, it is designed using the system deviations optimization. The STATCOM output voltage is controlled either by conventional PID or by ANN controllers to compare the results. The ANNs main task is to adapt the controller parameters to the operating condition. The simulation results show the adaptability, robustness, reliability and the effectiveness of the ANN-STATCOM controller to provide significant damping characteristics over the conventional controller for various disturbances at a wide range of operating conditions.

5. APPENDICES

Appendix-A

Superconducting Generator Parameters:

2000 MVA, 1700 MW, 3000 rpm

$X_d=X_q=0.5457$ p.u., $X_{D1}=X_{Q1}=0.2567$ p.u.

$X_{D2}=X_{Q2}=0.4225$ p.u., $X_f=0.541$ p.u., $R_a=0.003$ p.u.

$X_{fd}=X_{fD1}=X_{dD1}=X_{dD2}=X_{D1D2}=0.237$ p.u.

$X_{qQ1}=X_{qQ2}=X_{Q1Q2}=0.237$ p.u., $X_{fD2}=0.3898$ p.u.

$R_{D1}=R_{Q1}=0.1008$ p.u., $R_{D2}=R_{Q2}=0.00134$ p.u.

Field time constant=750 sec., H=3 KW.s/KVA.

Transmission line parameters:

$X_T=0.15$ p.u., $R_T=0.003$ p.u., $X_L=0.195$ p.u., $R_L=0.0075$ p.u.

Turbines And Governor System Parameters:

$T_{HP}= T_{GM}=0.1$ s, $F_{HP}=26\%$, $T_{IP}=0.1$ s, $F_{IP}=42\%$

$T_{LP}=0.3$ s, $F_{LP}=32\%$, $T_{HR}=10$ s, $P_O=1.2$ p.u.

SCG's PID Controller Parameters:

$K_p=0.18266$, $K_i=0.0001257$, $K_d=0.072285$.

STATCOM Parameters in SMIB System:

$G_s=1/28$ p.u.;$C_s=1$ p.u., $K_s=0.9$ p.u.

DC voltage regulator: $K_{pv\phi}=20.642$, $K_{iv\phi}=13.359$

AC voltage regulator: $K_{pvc}=2.0273$, $K_{ivc}=0.1592$

damping controller PID_ϕ: $K_{p\phi}$=1.0351, $K_{i\phi}$=1.1995, $K_{d\phi}$=0.00456
damping controller PID_c: K_{pc}=0.4372, K_{ic}=1.6878, K_{dc}=0.01096

STATCOM parameters in muli-machine System

G_s=1/28 p.u.;C_s=1 p.u., K_s=0.9 p.u.
K_{pc}=0.19024, K_{ic}=0.39253, K_{dc}=0.00207
$K_{p\phi}$=0.44093, $K_{i\phi}$=0.71248, $K_{d\phi}$=0.0063
$K_{pv\phi}$=0.71002, $K_{iv\phi}$=0.33503
K_{pvc}=0.39921, K_{ivc}=0.62223

Table 4 Conventional machines parameters

Unit	G_1	$G_{3,4,7}$	$G_{5,8}$	G_6	G_9	G_{10}
Rated (MVA)	920.35	835	615	896	1070	410
X_d (p.u.)	1.7900	2.1830	0.8979	1.7900	1.933	1.7668
$X_d^{'}$ (p.u.)	0.3550	0.4130	0.2995	0.2200	0.4670	0.2738
X_q (p.u.)	1.6600	2.1570	0.6460	1.7150	1.7430	1.7469
$X_q^{'}$ (p.u.)	0.5700	1.2850	0.6460	0.4000	1.1440	1.0104
$T_{do}^{'}$ (s)	7.9000	5.6900	7.4000	4.3000	6.6600	5.4320
H (s)	3.7638	2.6424	5.148	2.9297	3.0953	3.7041
K_d (p.u.)	2.00	2.00	2.00	2.00	2.00	2.00

Table 5 Excitation systems and PSSs parameters

Unit	G_1	$G_{3,4,7}$	$G_{5,8}$	G_6	G_9	G_{10}
K_A (p.u.)	25.000	400	200	250	400	400
T_A (s)	0.20	0.02	0.02	0.20	0.02	0.02
K_F (p.u.)	0.084	0.030	0.010	0.036	0.060	0.030
T_F (s)	1.00	1.00	1.00	1.00	1.00	1.00
E_{fdmax} (p.u.)	4.31	5.02	7.32	5.15	4.80	3.29
E_{fdmin} (p.u.)	-4.31	0.00	0.00	-5.15	0.00	0.00
G_S (p.u.)	0.03	0.03	0.03	0.03	0.03	0.03
T_1 (s)	0.15	0.15	0.15	0.15	0.15	0.15
T_2 (s)	0.015	0.015	0.015	0.015	0.015	0.015

References:

[1] E. Acha, et al, "Power Electronic Control in Electrical Systems", NEWNES power engineering series, ISBN 0 7506 5126 1, 2002.

[2] M. S. ElMoursi, "Flexible AC Transmission FACTS-Technology and Novel Control Strategies for Power System Stabilization Enhancement", Ph. D. thesis, University of New Brunswick, May 2005.

[3] V. K. Sood, "HVDC and FACTS Controllers: Applications of Static Converters in Power Systems", Book published by Kluwer Academic press, e- ISBN: 1-4020-7891-9, 2004.

[4] X. P. Zhang, C. Rehtanz and B. Pal, "Flexible AC Transmission Systems: Modelling and Control", ISBN-10 3-540-30606-4, Springer-Verlag Berlin Heidelberg, 2006.

[5] A. Jain, et al, "Voltage Regulation With STATCOMs: Modeling, Control and Results, IEEE Transactions on Power Delivery, vol. 21, No. 2, pp. 726-735, April 2006.

[6] K. R. Padiyar, V. S. Prakash, "Tuning and performance evaluation of damping controller for a STATCOM", Electrical Power and Energy Systems, vol. 25, pp.155–166, 2003.

[7] S. F. Faisal, A. H. M. A. Rahim, J. M. Bakhashwain, "A Robust STATCOM Controller for a Multi-Machine Power System Using Particle Swarm Optimization and Loop-Shaping", International Journal of Electrical, Computer, and Systems Engineering ,vol. 1 No. 1, ISSN 1307-5179,pp. 64-70, 2007.

[8] S. M. Osheba et al, "Comparison of transient performance of superconducting and conventional generators in a multimachine system", IEE-Proc. 135, pt. C, No. 5, pp.389-395, September 1988.

[9] H. A. Khattab, "Stabilization of A Superconducting Generating Unit In A Multi-machine System", Ph.D. Thesis, Menoufia University, Faculty of Eng. 2007.

[10] G. A. Morsy, H. A. Kattab and A. Kinawy, "Design of a PI controller for a superconducting generator", Eng. Research. Vol. 23, No. 1, Fac. of Eng., Men., Univ., pp. 61-77, January 2000.

[11] H. A. Khattab, "Control and Performance Analysis of A Superconducting Generator", M.Sc. thesis, Menoufia University, Faculty of Eng., 2000.

[12] M.A. Abido, "Analysis and assessment of STATCOM-based damping stabilizers for power system stability enhancement", EPSR, vol. 73, pp. 177–185, 2005.

[13] G. P. Chen, O. P. Malik, et al, "An Adaptive power system stabilizer based on the self-optimizing pole shifting control strategy", submitted to IEEE/PES winter meeting 1993.

[14] M. JUAN, et al, "Neural Network Control of the STATCOM in Multimachine Power Systems", WSEAS Transactions on Power Systems, Issue 9, Volume 2, pp. 209-214, ISSN 1790-5060, September 2007.

[15] Y. Zhang et al, "An artificial neural network based adaptive power system stabilizer", IEEE Trans. on EC-8. No. 1, pp. 71-77, March 1993.

[16] G. K. Venayagamoorthy, et al, "Implementation of adaptive critic-based neurocontrollers for turbogenerators in a multimachine power system", IEEE Trans. Neural Networks, vol. 14, No. 5, pp. 1047-1064, 2003.

[17] N.C. Sahooa et al, "Application of a multivariable feedback linearization scheme for

STATCOM control", Electric Power Systems Research, Vol. 62, Issue 2, pp 81-91, 2002.

[18] R. A. Saleh, "Transient Voltage analysis and control of a superconducting Generator", M.Sc. thesis, Egypt, Menoufia University, Faculty of Engineering, 1993.

[19] R. A. Amer, "Artificial Intelligence Control for a Superconducting Generator in a Multimachine Power System", M.Sc. thesis, Egypt, Menoufiya University, Faculty of Engineering, 2007.

[20] G. A. Morsy, R. A. Amer and H. A. Yassin, "A New Unsupervised ANN Based PID Controller for a Superconducting Generator", Eng. Research. Fac. of Eng., Men., Univ., Vol. 30, No. 4, pp.409-416, October 2007.

[21] Y. Y. Hsu and C. J. Wu, "Design of PID Static VAR Controllers for The Damping Of Subsynchronous Oscillations", submitted to IEEE/PES summer meeting 1987.

[22] M. A. Pai, "Energy Function Analysis for Power System Stability", Kluwer, 1989

[23] Yao-nan Yu, "Electric Power System Dynamics", New York: Academic Press, 1983.

[24] A. H .El-abiad, "Power systems analysis and planning", Purdue University, West Lafayette, Indiana USA, 1983.